Systems Microbiology and Biomanufacturing (2023) 3:370–383
https://doi.org/10.1007/s43393-022-00108-5

ORIGINAL ARTICLE

Nitrate removal from groundwater using chemically modified coconut husk based granular activated carbon: characterization of the adsorbent, kinetics and mechanism

Solomon K. M. Huno[1,2] · Jewel Das[3,4] · Eric D. van Hullebusch[1,5] · Ajit P. Annachhatre[2,6] · Eldon R. Rene[1]

Received: 25 February 2022 / Revised: 29 April 2022 / Accepted: 4 May 2022 / Published online: 1 July 2022

Abstract

In this study, a highly porous chemically activated granular activated carbon (GAC) was prepared from coconut husk and tested as an adsorbent to remove nitrate from contaminated groundwater. The prepared GAC was characterized by Fourier-transform infrared spectroscopy (FTIR), thermogravimetric and differential thermal analysis (TGA/DTA), scanning electron microscopy (SEM) and the Brunauer–Emmett–Teller (BET) surface area (S_{BET}) analysis. The effects of various process parameters such as initial nitrate concentration, contact time and adsorbent dose on nitrate removal efficiency (response) by the modified GAC were investigated using the statistically significant response surface methodology and Box–Behnken design of experiments. The experimental data were fitted to well-known adsorption isotherms and kinetic models to ascertain the mechanism of the adsorption process. Analysis of variance (ANOVA) was performed to determine the significance of the individual and the interactive effects of process variables on the response. The BET surface area (S_{BET}) and micropore volume of the prepared GAC from coconut husk was 1120 m^2/g and 0.392 cm^3/g, respectively. The experimental results showed that physisorption was the main adsorption mechanism governing the process, while the rate of adsorption was limited at initial nitrate concentrations > 10 mg/L. The Langmuir mono-layer adsorption isotherm best fitted the experimental data with a maximum adsorption capacity of 6.0 ± 1.3 mg/g (~92.5%) with an adsorbent dose of 0.1 g/50 mL, an equilibrium time of 6 h at 28 ± 2 °C, and at pH 7.6 (± 0.2). Among the tested process variables, the adsorbent dose and initial nitrate concentration showed significant effects on the nitrate removal efficiency.

Graphical abstract

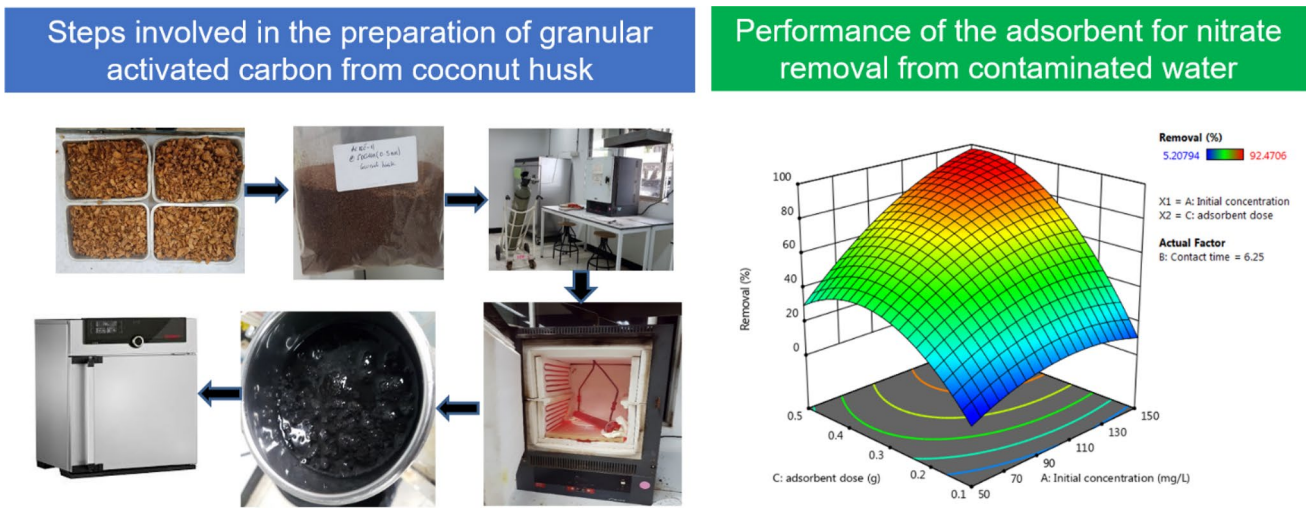

Extended author information available on the last page of the article

Keywords Nitrate adsorption · Groundwater · Granular activated carbon · Response surface methodology (RSM) · Box–Behnken · Coconut Husk

Introduction

Nitrate pollution of groundwater from both geogenic sources and anthropogenic sources such as wastewater, animal manure, leaky septic systems, and particularly nitrogen fertilizers from agricultural production, has raised concerns globally due to the probable challenges it may render to groundwater resource use [3, 7, 26, 33, 38, 65, 66, 74, 84]. Elevated nitrate concentrations in groundwater represent potential adverse effects to human health when ingested [1, 14, 58, 61, 67, 77]. Long-term ingestion of water with elevated nitrate concentrations (i.e. > 50 mg/L) may contribute to the development of *methemoglobinemia*, also called the "blue baby syndrome", colorectal cancer, bladder cancer, and gastrointestinal irritations in humans and fetal deformation in animals [20, 40, 78] The World Health Organization (WHO) has set drinking water standards for nitrate as 50 mg/L or 11.3 mg/L NO_3^-–N [75, 76].

Nitrate-contaminated groundwater may be treated by biological, chemical, electrochemical, and physico-chemical methods, or their combinations, typically involving different processes including biological denitrification, chemical denitrification, catalytic nitrate reduction, ion exchange, membrane bioreactors, reverse osmosis, and adsorption [1, 18, 33, 63, 85]. The selection of any of these methods for nitrate removal largely depends on the combination of factors including the operation cost, maintenance needs of the system, energy demands, efficiency, and the need for secondary treatment [34, 48]. Adsorption-based processes are widely applied to remove various contaminants, including nitrate from aqueous media mainly due to their efficiency, low cost, low maintenance requirements, simplicity of design, and convenience of operation [11, 60]. Adsorption-based nitrate removal processes benefit from the flexibility of obtaining highly porous adsorbents from a range of materials such as industrial wastes [10, 80], chitosan beads [70], silica [40, 41], nano-alumina [23], clay [9], zeolites [51, 43], and agricultural wastes [52]. Locally available lignocellulosic wastes such as coconut husk have good potentials for producing highly porous low-cost adsorbent for the removal of pollutants from the aqueous mediums [48, 71, 72]. The use of coconut husk for preparing activated carbon provides useful alternatives for the application of coconut husk in major coconut-producing countries like Brazil, India, Thailand, Indonesia, the Philippines, and Sri Lanka that often have to deal with the organic matter disposal as well as copious phenolic compound emissions from these wastes [13, 47, 54, 55].

Numerous adsorption studies have favored activated carbon adsorbents due to their favorable surface chemistry for nitrate adsorption, high porosity, and surface area. However, their adsorption capacity can be influenced by process parameters such as initial nitrate concentration, contact time, pH, temperature, adsorbent dose, and also the interaction effects of these parameters [11, 24, 48, 56, 69, 80]. For example, high nitrate removal rates may be achieved for high initial nitrate concentration (ca. 100–450 mg/L), while adsorption capacity generally decreases with an increase in the pH [4, 19, 21, 44, 53, 81].

Few studies have investigated the potential application of coconut husk-based activated carbon applications for nitrate removal from groundwater. In this study, the mechanism of nitrate removal from groundwater onto chemically modified coconut husk-based granular activated carbon was tested based on experimental nitrate sorption kinetic data as well using isotherm models to fit the experimental data. Response Surface Methodology (RSM) was employed for the optimization of the experimental design process, along with a simultaneous and systematic estimation of the effect of different process parameters. RSM combined with a suitable design of experiment helps to optimize processes with minimum experimental run, at a comparatively low cost [15, 40, 72, 83]. In addition, the interaction effects of process parameters of adsorption and their non-linear influence on the adsorption efficiencies of nitrate ions onto the activated carbon prepared from coconut husk were investigated in order to fill a gap in the literature and contribute to the current understanding of nitrate adsorption by lignocellulosic materials.

Materials and methods

Preparation of K_2CO_3 treated granular activated carbon (GAC) from coconut husk

Locally obtained coconut husk was thoroughly washed and sun-dried for 2 weeks. The dried coconut husk (precursor) was further oven dried for 24 h to remove the residual moisture and other volatile impurities. The husk was then crushed and reduced to smaller particle size fractions. Standard sieves (ASTME-11) were used to reduce the dried coconut husk to average particle sizes ranging between 0.315 and

0.710 mm. Chemical impregnation was achieved by mixing of the sieved raw precursor with reagent grade K_2CO_3 (99% purity, Ajax Finechem) at a mass ratio of 1 (mass of precursor: mass of K_2CO_3) and equal amount of water according to Eq. 1. The impregnated sample was dried in an oven (UF 110, Memmert GmbH + Co. KG, Germany) for 24 h at 105 °C. Afterwards, the sample was loaded in a tubular stainless-steel reactor and carbonized in a programmable muffle furnace to 800 °C for 2 h with nitrogen gas flow at 15 L/min. The activated carbon was then washed several times with de-ionised water to neutralize the pH.

$$\text{Impregnationratio, IR} = \frac{w_{K_2CO_3}}{w_{\text{char}}}, \tag{1}$$

where $w_{K_2CO_3}$ is mass of K_2CO_3 in gram and w_{char} is mass of char (g).

The yield of the K_2CO_3 activated carbon was determined according to Eq. 2.

$$\text{Yield} = \frac{m_{\text{AC}}}{m_{\text{HUSK}}}, \tag{2}$$

where m_{AC} is mass of activated carbon after carbonization in gram, and m_{HUSK} is the mass of raw coconut husk in grams before carbonization.

Characterization of the adsorbent materials

The moisture content, volatile matter, ash content, and fixed carbon content of the raw precursor, and K_2CO_3 impregnated coconut husk, and the prepared activated carbon adsorbent were analyzed using a thermogravimetric analyzer, TGA 701 (LECO Co., USA). The prepared granular activated carbon adsorbent was analyzed with Fourier transform infra-red spectroscopy (FTIR) analyzer (Thermo-scientific, Nicolet™ 6700 model) to determine the functional groups present on the surface of the adsorbent. The surface morphology of the prepared granular activated carbon was determined with a scanning electron microscope, SEM (Model: HITACHI S-3400N, Japan). A thermal analyzer (STA449, Netzsch, Jupiter) was used to examine the thermogravimetric and differential thermal properties of the K_2CO_3 impregnated coconut husk at process conditions similar those used during the preparation of the granular activated carbon. The K_2CO_3 impregnated precursor was heated to 800 °C from room temperature (~ 25 °C), at a heating rate of 10 °C/min (as applied during the carbonization of sample), with a nitrogen flow rate of 15 L/min. The differential thermal analysis provides insight into the effect of the chemical activation agent, K_2CO_3, on the decomposition of hemicellulose, cellulose, and lignin fractions present in the precursor.

The specific surface area of the prepared granular activated carbon was analyzed with a Quantachrome (NOVA 2200 series) volumetric gas adsorption equipment. Single-point nitrogen adsorption data were generated in the relative pressure range of 0.009–0.6 at − 196 °C. The Brunauer–Emmett–Teller surface area (S_{BET}) was determined within the relative pressure ($p/p°$) range of 0.009–0.3. The pore characteristics such as median pore width, pore distribution, and the total pore volume of the adsorbent was examined using the density functional theory (DFT) approach, Barrett–Joyner–Halenda (BJH) method, and micro pore (MP) method, respectively [59]. The calculated values were compared with the measured values to determine the goodness of fit and the reliability of the generated data.

Preparation of the groundwater sample

Groundwater sample was collected from a borehole located at Khlong Suang in the Pathumthani province of Thailand following the standard groundwater sampling protocols [79]. Groundwater sample was filtered using 0.45 µm membrane filter and stored in refrigerator at 4 °C. Groundwater samples were spiked with KNO_3 salt (99% purity, Ajax Finechem) to produce groundwater solution of nitrate concentration 10, 50, and 150 mg/L, at initial an pH of 7.6 (± 0.2). Background nitrate concentration in the groundwater was determined using the UV spectrophotometric screening method (4500-NO_3^-) [6] and after spiking with KNO_3.

Experimental design and adsorption modelling

Design of experiments

Nitrate removal yield (%) with the highly porous chemically modified granular activated carbon (GAC) prepared from coconut husk was evaluated as a function of the following three independent process parameters: initial groundwater nitrate concentration, contact time and adsorbent dose at boundary conditions (i.e. fixed conditions) of pH 7.6 (± 0.2) and temperature of 28 (± 2) °C. Experimental levels of the process parameters were selected based on the experimental boundaries, i.e. the polluted groundwater nitrate concentrations, average groundwater pH, maximum contact time, and ambient temperature, based on results from preliminary screening batch experiments and from the literature. To eliminate unnecessary experimental runs and yet retain the relevant experiments in the matrix of the experimental design, RSM and Box–Behnken coupled design of experiment was used to model and optimize the nitrate adsorption process.

The Box–Behnken experimental design was used to design a 3-factor, 3-level experimental design, while RSM was used to optimize the experiment design by systematically varying all variables to yield a well-designed experiment with minimum number of experimental runs [8]. The

Table 1 Experimental levels and ranges of independent process parameters

Variable	Units	Range and levels		
		Low level (−1)	Center level (0)	High level (+1)
A: x_1, initial concentration	mg/L	50	100	150
B: x_2, contact time	h	0.5	6.25	12
C: x_3, adsorbent dose	g/100 mL	0.1	0.3	0.5

behavior of the adsorption process was further modeled by a second-order polynomial regression model of the quadratic response model. The minimum and maximum limits of the experimental variables calculated according to Eq. 3 are shown in Table 1. The Design Expert software (version11, STATEASE Corp. USA) was used to aid the generation of the experimental runs, regression analysis, and optimization of the process variables to achieve the response, as well as estimate the statistical significance of the model equations.

$$x_i = \left(\frac{z_i - z_i^{\,0}}{\Delta z_i}\right)\beta_{\mathrm{d}}, \tag{3}$$

where z_i is the real value of independent variable, Δz_i is the distance between the real value in the central point and the real value in the superior or inferior level, β_{d} is the coded limit value of the experimental matrix for the given variable and z_i^0 the real value at central point.

A response surface methodology (RSM)-based approach was applied to model the relationship between the nitrate removal (response) and a set of independent variables (*A*: initial concentration of nitrate in groundwater, *B*: contact time, and C: adsorbent dose) using the following quadratic equation (Eq. 4):

$$Y = \beta_{\mathrm{O}} + \sum \beta_i x_i + \sum \beta_{ii} x_{ii}^2 + \sum \beta_{ij} x_i x_j + \varepsilon, \tag{4}$$

where Y is the predicted response, i.e., the percentage removal for nitrate, β_{o} is the constant coefficient, β_i is the ith linear coefficient of the input factor x_i, β_{ii} is the ith quadratic coefficient of the input factor x_i, β_{ij} is the different interaction coefficients between the input factors x_i and x_j, and ε is the error of the model.

The model was evaluated using analysis of variance (ANOVA) to test the quality of the model [64, 83]. The significance of the model terms and the goodness of the quadratic model fit with the experimental data (i.e. for nitrate removal efficiency) were determined by the F- values, the p-values, and the correlation coefficient (R^2) [2, 62].

Batch adsorption experiments

To examine the nitrate adsorption capacity of the coconut husk-based GAC, batch experiments were carried out by adding 0.1 g of the prepared granular activated carbon adsorbent into a 250-mL Erlenmeyer flask containing 50 mL nitrate-contaminated groundwater and using three different initial nitrate concentrations (10, 50 and 150 mg/L). The pH and temperature of each treatment were maintained at 7.6 (±0.2) and 28 (±2) °C, respectively. The experimental flasks were placed on a programmable temperature-controlled orbital shaker (DATHAN scientific Co.) at a mixing speed of 180 rpm. To study the nitrate adsorption capacity of the activated carbon with time, the samples were collected periodically at 0.5, 1.0, 1.5, 2.5, 3.0, 3.5, 6, 9 and 12 h and filtered through a 0.45-µm filter. The residual nitrate concentration in the filtrate was measured using a UV-spectrophotometer (HITACHI, U-2900). To ensure reproducibility, and for statistical reasons, all the experiments and the measurements were performed in triplicates. The experimental data were evaluated for sources of systematic errors and potential uncertainties introduced in the results due to random errors were limited as much as possible.

Adsorption isotherm studies

To evaluate the efficacy of the coconut husk-based granular activated carbon for nitrate removal, the equilibrium adsorption of nitrate from groundwater was studied as a function of the initial nitrate concentration. The Langmuir isotherm and Freundlich isotherm were used to describe the experimental data and for equilibrium modelling. The linearized form of the Langmuir equation (Eq. 5) is given as follows:

$$\frac{1}{q_{\mathrm{e}}} = \frac{1}{q_{\mathrm{m}}} + \frac{1}{q_{\mathrm{m}} b C_{\mathrm{e}}}, \tag{5}$$

where q_{e} is the amount adsorbed at equilibrium concentration, C_{e}. q_{m} is the Langmuir constant representing maximum monolayer adsorption capacity, and b is the Langmuir constant related to energy of adsorption. This model implies that saturation of the adsorptive surface is possible; thus, q_{e} eventually can reach a maximum value (q_{m}).

$$R_{\mathrm{L}} = \frac{1}{1 + K_L \mathrm{C_o}} \tag{6}$$

Adsorption favorability was determined by calculating the separation constant, R_{L} [44, 22], and dimensionless factor was calculated according to the Eq. 6. K_{L} refers to the Langmuir constant and C_{o} refers to the initial adsorbate concentration.

The linearized form of the Freundlich isotherm is shown in Eq. 7.

$$\log q_e = \log K_f + \frac{1}{n}\log C_e, \tag{7}$$

where q_e and C_e are the same as in Eq. 5, and K_f and n relate to the capacity and intensity of adsorption, respectively. The Freundlich model does not imply a saturation of the adsorptive surface.

Adsorption kinetic studies

The kinetic models, pseudo-first order (Eq. 8) and pseudo-second order (Eq. 9) were used to study the adsorption mechanism based on the experimental data [31, 39].

$$\frac{dq_t}{dt} = k_1\left(q_e - q_t\right), \tag{8}$$

$$\frac{dq_t}{dt} = k_2(q_e - q_t)^2, \tag{9}$$

where q_e and q_t are the amounts of nitrate adsorbed (mg/g) at equilibrium and at time t (h), respectively; k_1 is the rate constant of the pseudo-first order adsorption (min^{-1}); and k_2 is the rate constant of the pseudo-second order adsorption (g/mg/min).

In batch experiments, nitrate removal from groundwater by the adsorbent was estimated according to Eq. 10.

$$R(\%) = \frac{C_i - C_e}{C_i} \times 100\% \tag{10}$$

At equilibrium conditions, the nitrate removal capacity by the adsorbent was calculated according to Eq. 11:

$$q_e = \frac{\left(C_i - C_e\right) \times V}{m_{ads.}}, \tag{11}$$

where C_i = initial concentration in the bulk solution (g/L), C_e = equilibrium concentration in the bulk solution (g/L), V = volume of the solution (mL), m_{ads} = mass of the adsorbent (g), and R = removal efficiency (%).

Results and discussion

Characteristics of the absorbent materials

The raw coconut husk and K_2CO_3 impregnated coconut husk showed comparatively high volatile matter content of ~ 65.0 (± 0.8) % (wt.) and ~ 46.4 (± 0.3) % (wt.), respectively, as shown in Table 2. However, the K_2CO_3 impregnated coconut husk had the highest ash content. The highest amount of fixed carbon was observed in the K_2CO_3 coconut husk granular activated carbon. Consistent with the findings of Suman and Gautam [71], the higher fraction of ash content yielded the lowest values of fixed carbon in the K_2CO_3 impregnated coconut husk, which in this case, may be attributed to the unreleased intercalated potassium which does not get easily released at temperatures below 600 °C, but incorporated in the ash [74].

Thermogravimetric analysis (TGA) of the raw material

Thermal gravimetric analysis (TGA) and differential thermal analysis (DTA) provide insight into the composition and thermal stability of the raw material by examining the thermo-chemical weight loss and the decomposition kinetics associated with the thermal degradation of the hemicellulose, cellulose, and lignin fractions of K_2CO_3 impregnated coconut husk. The results of the TGA/DTA analysis are shown in Figure S2. An initial weight loss of 42.5% (6.72 mg) which peaked at 257 °C corresponds to the combined loss of the adsorbed moisture and an initial devolatilization initiated at 152 °C which peaked at 257 °C. The light gases such as CO, CO_2 and CH_4 for cellulose, hemicellulose and lignin, respectively, are released at this stage [73, 82]. This is corroborated by the corresponding weight lost within the 152 °C and 257 °C temperature regime that exceeds the weight of measured moisture content of the sample as shown in Table 2. Subsequently, the decomposition of hemicellulose and cellulose fractions was observed to occur within a temperature range of 257–302 °C, comparable to about 28%

Table 2 Characterization of raw coconut husk, K_2CO_3 impregnated coconut husk, and activated carbon

Parameter	Raw coconut husk	K_2CO_3 impregnated coconut husk	Activated carbon
Volatile matter content (%)	65.0 ± 0.8	46.4 ± 0.3	15.4 ± 0.1
Moisture content (%)	8.4 ± 0.1	6.8 ± 0.1	21.6 ± 0.1
Ash content (%)	3.9 ± 0.1	39.8 ± 1.7	3.8 ± 0.1
Fixed carbon content (%)	22.8 ± 0.7	7.1 ± 1.4	59.3 ± 0.1

weight loss at the second half of the DTA curve. Within this temperature range, the thermal decomposition of cellulose fractions with structural compositions of long polymers of glucose, which are more stable than the hemicellulose fractions would occur. This finding is corroborated by previous studies from the literature which asserts that the decomposition of hemicellulose occurs in biomass pyrolysis only after 200 °C, mainly because of the presence of amorphous structures [25, 27, 32, 42, 49]. Thermal degradation of lignin, however, was characterized by a relatively slower weight loss rate which started from 302 to 550 °C. The observed slower thermal degradation rate is attributable to the complex molecular structure of the lignin fractions [86]. Thermal decomposition and volatilization of the various fractions of the K_2CO_3 activated coconut husk results in a higher carbon content (% wt.) activated carbon with higher porosity and adsorption capacity than the raw coconut husk, since moisture, volatiles, and non-carbon heteroatoms were removed during the process of thermal treatment.

Surface morphology of the granular activated carbon prepared from coconut husk

The surface characteristics of the activated carbon show a rough surface with mixed pore types and a circular aperture but distorted geometry (Figure S3 a–d). These porous structures or pores formed on the surface of the prepared coconut husk granular activated carbon were created during the reactions between the raw coconut husk and K_2CO_3, and the release of reaction gases and volatile matter during the carbonization and the chemical activation process. The presence of the pore structures, i.e. macropores, micropores and mesopores, on the prepared coconut husk activated carbon makes it a suitable adsorbent for effective nitrate ion adsorption from the aqueous medium. However, the macropores frequently function as transmitters without any adsorption potential, whereas the micropores and mesopores are excellent sites for nitrate ion adsorption [25].

Pore distribution and S_{BET} of K_2CO_3 granular activated carbon prepared from coconut husk

Various methods are used to modify and improve the nitrate adsorption capacity of adsorbents by increasing their porosity, active sites and the positive surface charge [49]. Base (e.g. KOH, NaOH or K_2CO_3) treated activated carbon has been reported to have high surface area (generally greater than 1000 m^2/g) [30], with an average carbon yield of ~ 35%. The Brunauer–Emmett–Teller surface area was determined as 1120 m^2/g and the micropore volume as 0.392 cm^3/g. The measured median pore width of the K_2CO_3 coconut husk_activated carbon was 0.755 nm and the single-point desorption total pore volume (of pores less than 40.31122 nm width at $p/p^\circ = 0.9500$) was found to be 0.459 cm^3/g (Table 3).

The pore development and distribution on the highly porous activated carbon produced from coconut husk was mainly influenced by the activation agent and the activation temperature. The intensity of heating enhances the reaction between K_2CO_3 and the coconut husk components [5]. At higher heating rates up to 627 °C, alkali metal ions were removed from the intercalation developed during chemical impregnation [29, 35]. Elimination of the alkali ions results in the development of increased surface area and pore diameter [50]. K_2CO_3 reduces to K_2O and CO_2 according to the equation (Eq. 12–13). However, at temperatures beyond 627 °C, the char produced exhibits significant weight loss due to the reaction of K_2O and C (Eq. 14) [59].

$$K_2CO_3 + 2C \rightarrow 2K + 3CO, \tag{12}$$

$$K_2CO_3 \rightarrow K_2O + CO_2, \tag{13}$$

$$K_2O + 2C \rightarrow 2K + CO. \tag{14}$$

Table 3 Surface properties of K_2CO_3 modified coconut husk derived granular activated carbon

Property	Unit	Value
Yield	%	35.1
Micro pore volume	cm^3/g	0.392
Surface area, S_{BET}	m^2/g	1120
Median pore width	nm	0.755
Total pore volume	cm^3/g	0.459

Table 4 FTIR frequencies of adsorbent before adsorption

Peak (cm^{-1})	Functional group
3423	hydroxyl compounds
2918	Methyl
2815	Methylene
1740	Carbonyl
1566	C=C in aromatic rings
1380	C−O in acids, ethers, alcohols, phenols, esters

FTIR of the granular activated carbon prepared from coconut husk

The FTIR spectra analysis of the granular activated carbon from coconut husk (Figure S4 and Table 4) exhibited a broad adsorption band of about 3650–900 cm^{-1}. The peak of 3423 cm^{-1} with broad band range of 3550–3300 cm^{-1} is typical characteristic of the stretching vibrations of hydroxyl compounds. The bands at 2918 cm^{-1} and 2851 cm^{-1} showed the presence of asymmetric C–H and symmetric C–H bands of the methyl and methylene groups. The weak peak around 1740 cm^{-1} can be attributed to the stretching of carbonyl C = O present in ketones, aldehyde, esters, and acetyl derivatives. Furthermore, the band located at 1566 cm^{-1} was ascribed to the stretching vibrations of C=C in the aromatic rings. The peak at 1380 cm^{-1} as assigned to C–O stretch in acids, alcohols, phenols, ethers, and esters [25, 81]. The K_2CO_3 modified activated carbon produced from coconut husk exhibited the presence of acidic and basic functional groups.

Response surface methodology and optimization

Nitrate removal (%) from aqueous medium as a function of the following three process parameters: initial groundwater nitrate concentration, contact time, and adsorbent dose at ambient temperature (28 ± 2 °C) and pH of 7.6 (± 0.2), was investigated. The response, nitrate removal (%) for various experimental combinations of process parameters derived from the Box Behnken design is shown in Table 5.

Table 5 Experimental runs based on response surface methodology and Box–Behnken design of experiment

Un-coded values				
Run order	Initial conc. (mg/L) (*A*: x_1)	Contact time (h) (*B*: x_2)	Adsorbent dose (g/50 mL) (*C*: x_3)	Removal (%)
1	50	0.5	0.3	29.3
2	100	6.25	0.3	70.7
3	100	0.5	0.5	57.7
4	50	12	0.3	33.6
5	100	12	0.5	82.2
6	100	12	0.1	12.3
7	100	6.25	0.3	77.7
8	150	0.5	0.3	68.2
9	150	6.25	0.5	92.5
10	100	6.25	0.3	73.5
11	100	6.25	0.3	69.7
12	100	0.5	0.1	6.8
13	100	6.25	0.3	65.8
14	50	6.25	0.5	32.2
15	150	6.25	0.1	8.1
16	50	6.25	0.1	5.2
17	150	12	0.3	85.9

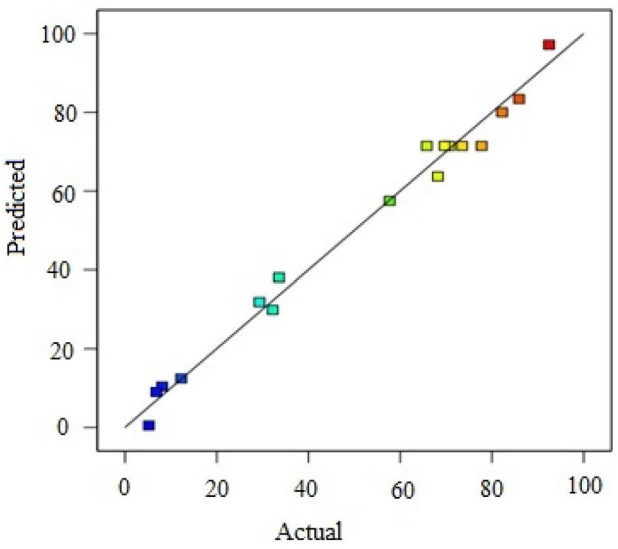

Fig. 1 Correlation between the predicted and the experimental removal efficiency for nitrate from groundwater by K_2CO_3 modified coconut husk granular activated carbon

The fitted regression model (Eq. 15) in real-term values was derived to understand quantitatively, the empirical relationships between the effects of varying process conditions and their interaction effects on the nitrate removal (%) from aqueous medium by the K_2CO_3 coconut husk granular-activated carbon:

$$Y = +71.49 + 19.30 + 6.48 + 29.02 + 3.36 + 14.35 + 4.77 - 11.25 - 5.98 - 25.75 \quad (15)$$

where Y is the nitrate removal efficiency (%) from groundwater by the K_2CO_3 granular activated carbon prepared from coconut husk, x_1 is the initial concentration in coded form, x_2 is the contact time in coded form and x_3 is the adsorbent dose in coded form.

The summary statistics of the quadratic regression model shows a predicted R^2 value of 0.8657 which is in reasonable agreement with the ''Adjusted R^2'' of 0.9699. The quadratic regression model of the nitrate removal (%) shows a statistically significant result which signifies the adequacy of the quadratic regression model to explain the relationship between the independent process variables and the response variable, i.e. the nitrate removal (%). The results of the predicted values of the model also correlate well (Fig. 1) with the measured actual values obtained for the run orders of the Box–Behnken experimental design.

Table 6 Multiple regression results and significance of the components for the quadratic model

Factor coded	Parameter	Coefficient	Standard error	*F* value	*p* value	SS	(PC %)
Intercept	β_0	71.49					
A: x_1	β_1	19.3	1.88	105.8	< 0.0001	2978.6	20.56
B: x_2	β_2	6.48	1.88	11.9	0.01	336.1	2.32
C: x_3	β_3	29.02	1.88	239.5	< 0.0001	6739.1	46.52
A^2: x_1^2	β_{11}	-11.25	2.59	1.61	0.0034	532.54	3.68
B^2: x_2^2	β_{22}	-5.98	2.59	29.3	0.0539	150.71	1.04
C^2: x_3^2	β_{33}	-25.75	2.59	3.2	< 0.0001	2791.0	19.27
AB: x_1x_2	β_{12}	3.36	2.65	18.9	0.2455	45.21	0.31
AC: x_1x_3	β_{13}	14.35	2.65	5.36	0.001	823.12	5.68
BC: x_2x_3	β_{23}	4.77	2.65	99.2	0.115	91.13	0.63

SS sum of squares, *PC* percentage contribution

The quality of the model was further tested by the analysis of variance (ANOVA) and the results were found to be significant with a p value < 0.0001 and F value of 58.23. The coefficient of determination (R^2) of the quadratic model was determined as 0.9887 which implies that only about 1.11% of the total variations was not explained by the model. The lack of fit of the model (F value > 0.05) was also determined to be non-significant, relative to the pure uncontrollable errors [40, 45].

The interaction effects of the independent variables on the nitrate removal efficiency (%) were evaluated by assessing the significance of the coefficients of the independent parameter effects based on their p values (Table 6). The positive coefficient values of the parameters indicate an increasing nitrate removal effect within the tested range while negative coefficients represent a reduction effect. The effect of initial concentration and adsorbent dose on nitrate removal efficiency was shown to have strongly influenced the nitrate removal efficiency compared to the contact time. The statistical test of significance suggests that initial concentration directly influenced the adsorption efficiency ($p < 0.0001$, $F = 105.8$). However, the quantified percent contribution (20.6%) by initial nitrate concentration of groundwater to the nitrate removal efficiency was found to be comparatively lower than the contribution of adsorbent dose ($p < 0.0001$, $F = 6739.1$ and PC = 46.5) to nitrate removal.

In physiochemical terms, this adsorption behavior suggests that increasing nitrate concentration for the same adsorbent dose increased the specific adsorption capacity, whereas increasing adsorbent dose increased the availability of adsorption sites for enhanced nitrate adsorption. An increase in the concentration of nitrate ions increases the likelihood of instantaneous adsorption of nitrate ions onto the available adsorption sites of the granular activated carbon.

Effect of adsorbent dose and initial nitrate concentration on nitrate removal from groundwater

Figure 2a–c shows the results of the 3D response surface plots and the interactive effects of initial nitrate concentration, contact time and adsorbent dose. The maximum adsorption efficiency of 92.5% was achieved at an initial concentration of 150 mg/L, contact time of 6.25 h and an adsorbent dose of 0.5 g/50 mL. The interaction effect of initial concentration, adsorbent dose and contact time shows a non-linear profile on the nitrate removal efficiency. At a constant initial concentration of 100 mg/L, the nitrate removal efficiency slightly increased with an increase in the adsorbent dose and contact time (Fig. 2a).

The rate of nitrate ion adsorption on to the K_2CO_3 modified activated carbon produced from coconut husk was observed to proceed rapidly at the initial stages of the experiment but it reduced gradually until equilibrium was attained. This may be explained by the increased availability of binding sites for instantaneous adsorption of nitrate ions onto the adsorbent. However, as the contact time increases beyond 6.25 h, the rate of uptake of nitrate ions from the solution reduced until equilibrium was attained. Similar results were reported by Battas et al. [9] and Madan et al. [45] for nitrate and α-toluic adsorption by local clay and CaO_2 nanoparticles, respectively. Compared to the adsorbent dose and initial nitrate concentration, the contact time showed the lowest influence on nitrate adsorption efficiency from groundwater.

The percent contribution of contact time (B: x_2) to nitrate adsorption (Table 6) from groundwater was quantified statistically as 2.3%, which is the lowest among the three process parameters though its effect on nitrate removal efficiency was statistically significant ($p = 0.01$). The effect of initial nitrate concentration on nitrate removal efficiency was observed to be statistically significant ($p < 0.0001$) contributing to about 20.6% effect on the nitrate adsorption efficiency. The adsorbent dose and initial nitrate concentration showed

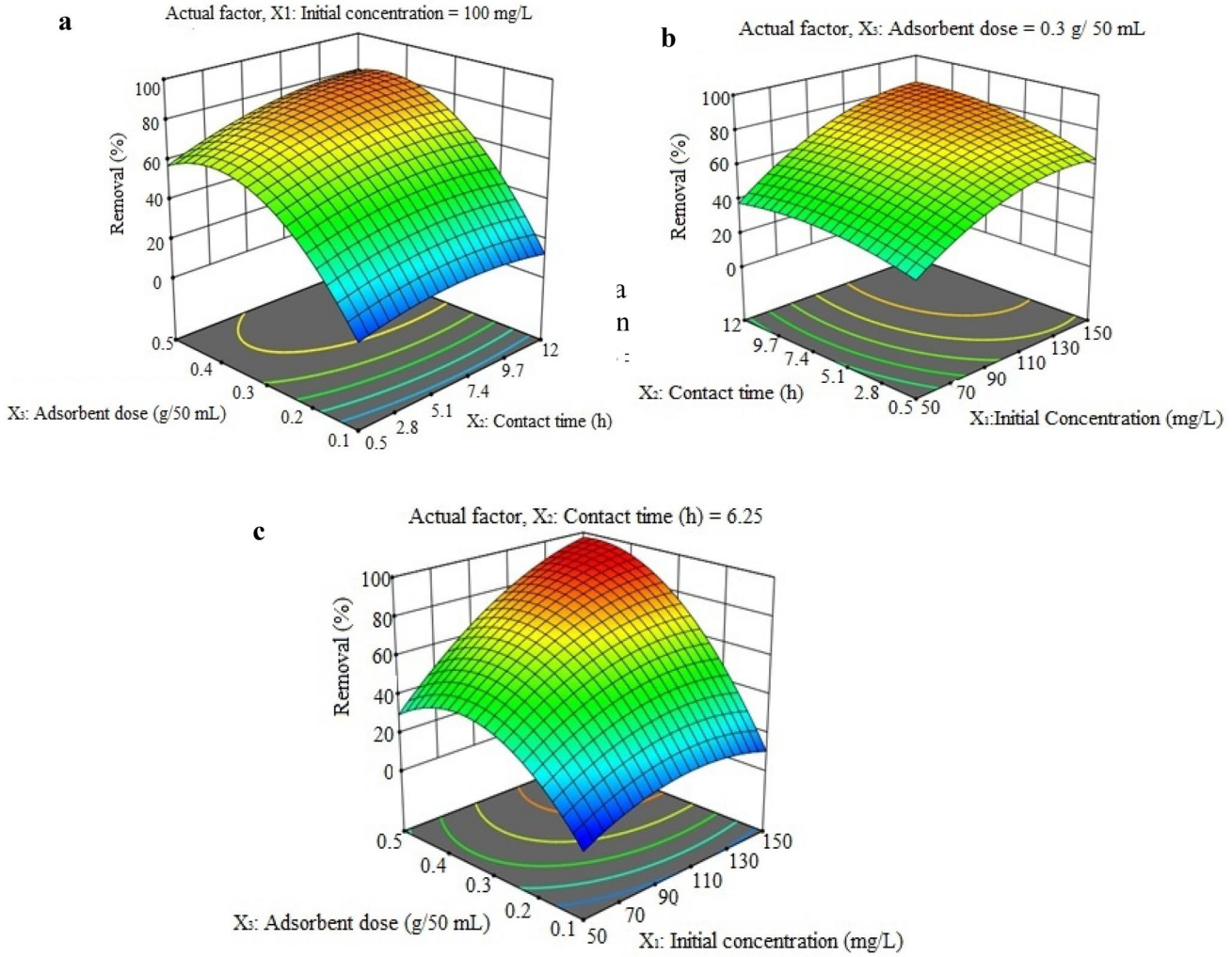

Fig. 2 Surface plots of removal efficiency (%) as a function of **a** adsorbent dosage and contact time; **b** contact time and initial nitrate concentration; **c** adsorbent dosage and initial concentration; at pH 7.6 ± 0.2 and temperature = 28 ± 2 °C and parity plot of the quadratic model

significant effects ($p < 0.0001$) on the nitrate removal from groundwater (Table 6).

At a fixed adsorbent dose (0.3 g/50 mL), the nitrate removal from groundwater by K_2CO_3 modified coconut husk granular activated carbon showed increased adsorption efficiency with increasing initial concentration and contact time until the maximum adsorption capacity of the adsorbent was attained (Fig. 2b). Similarly, at a fixed contact time of 6.25 h, high values of initial nitrate concentration and contact time increased the adsorption efficiency.

The adsorption mechanism may involve the immobilization of nitrate ions from solution onto the coconut husk GAC surface via weak bonds such as van der Waals forces, hydrogen bonding, or hydrophobic interactions. Nitrate ions are easily exchanged with the interlayer OH ions present on the surface of GAC activated carbon. Thus, the nitrate ions diffused until saturation condition is achieved at the micropores of the GAC. At saturation, the driving force for mass transfer of the adsorbates from the solution into the micro and mesopores of GAC has reported to reduce significantly due to the intermolecular repulsion between the adsorbate ions and the adsorbents surface [17]. Besides, as reported in several reports, the repulsive forces generated between nitrate ions on the adsorbent's surface prevented further nitrate ion uptake onto the activated carbon's surface [57, 68, 46].

Table 7 Pseudo-first order kinetic constants for nitrate adsorption form groundwater onto coconut husk granular activated carbon

Pseudo-first order kinetics					
Initial concentration (mg/L)	k_1 (min^{-1})	q_e (predicted) (mg/g)	q_e (experimental) (mg/g)	R^2	Normalized standard deviation, Δq_e (%)
10	0.031	0.08	0.10	0.993	34.3
50	0.028	0.51	1.04	0.880	
150	0.023	6.33	6.01	0.961	

Table 8 Pseudo-second order kinetic constants for nitrate adsorption from groundwater onto coconut husk granular activated carbon

Pseudo-second order kinetics					
Initial concentration (mg/L)	k_2 (g/mg min)	q_e (predicted) (mg/g)	q_e (experimental) (mg/g)	R^2	Normalized standard deviations Δq_e (%)
10	0.51	0.1	0.09	0.998	9.58
50	0.04	1.08	1.04	0.999	
150	0.002	6.9	6.0	0.987	

Adsorption kinetics

Nitrate adsorption from groundwater by granular activated carbon was studied as a function of the initial nitrate concentration of groundwater. The solid to liquid (S/L) ratio in the batch experiments were maintained at 0.1 g of granular activated carbon to 50 mL of groundwater solution. The temperature was maintained at 28 (± 2) °C and the pH at 7.6 (± 0.2). The results from the batch experiments for initial concentrations of 10, 50 and 150 mg/L were fitted to the pseudo-first order and pseudo-second order kinetic models to analyze the adsorption kinetics and the equilibrium conditions of nitrate adsorption from groundwater by K_2CO_3 modified coconut husk-activated carbon. The constants of the first-order kinetic model fitted the experimental data of the different concentrations as shown in Table 7. The pseudo-second order kinetic model constants were estimated by plotting t/q_t (h g/mg) versus time, t (min) for each of the initial concentrations. Table 8 shows the kinetic constants of the pseudo-second order kinetic model.

On the other hand, the R^2 values of the fitted pseudo-second order kinetic model for nitrate three concentrations (10, 50 and 150 mg/L) were high (> 0.98) and the model was able to describe the adsorption behavior of nitrate ions in groundwater onto K_2CO_3 modified coconut husk activated carbon.

Adsorption isotherm studies

The Langmuir and Freundlich isotherms were fitted to the experimental data in order to determine the interaction of nitrate ions present in groundwater with K_2CO_3 modified coconut husk granular activated carbon.

A linearized Langmuir isotherm model was plotted, i.e. $1/q_e$ versus $1/C_e$ and the Langmuir constants were obtained. The Langmuir constant, R_L, obtained for initial nitrate concentrations of 10, 50 150 mg/L were in the range of 0.2–0.8 (Table 9). A comparatively high regression coefficient of determination, R^2 value of 0.9332 was obtained (Table 9). The Freundlich constants shown in Table 9 were obtained from the slope of the linearized Freundlich model plot. The regression coefficient of determination, K_f and n values obtained for the Freundlich isotherm model were useful in describing the nature of the adsorption process and the adsorption affinity. The adsorption of nitrate ions from groundwater onto the granular activated carbon prepared from coconut husk followed a monolayer Langmuir isotherm model. The favored Langmuir isotherm model is a monolayer adsorption model based on the assumption that adsorption occurs by the sorption of adsorbates onto fixed number of localized sites on the adsorbent [48]. The maximum estimated Langmuir

Table 9 Langmuir and Freundlich coefficients for nitrate adsorption onto K_2CO_3 modified coconut husk GAC

Initial concentration (mg/L)	Langmuir isotherm parameters				Freundlich isotherm parameters		
	q_m (mg/g)	b (L/mg)	R^2	R_L	K_f (mg/g)(L/mg)$^{1/n}$	n_F	R^2
10	7.75	0.025	0.933	0.8	0.0993	1.151	0.753
50				0.444			
150				0.211			

adsorption capacity, q_m (mg/g) of the granular activated obtained, was also found to be very close to the experimental values.

The separation factor, (R_L) of the Langmuir model describes the favorability of the adsorption process where the value of R_L determines its favorability: unfavorable ($R_L > 1$), linear ($R_L = 1$), favorable ($0 < R_L < 1$) and irreversible ($R_L = 0$) [16, 28, 80]. In this study, the Langmuir constant, R_L was within the boundaries of $0 < R_L < 1$, which indicates a favorable adsorption process (Table 9). The values for R_L were observed to approach unity when the initial nitrate concentration increased. These adsorption conditions support the results that suggest the probable occurrence of instantaneous adsorption of the nitrate ions from the groundwater onto the surface of the granular activated carbon. This phenomenon was most favored at higher initial groundwater nitrate concentrations. The Freundlich isotherm model constant, n_F, obtained from the slope of the linear plot using experimental data from the adsorption experiment shows values greater than 1. The physical sorption processes are usually characterized by $n_F > 1$, while $n_F < 1$ and $n_F = 1$ denotes chemisorption and linear adsorption processes, respectively [17, 16]. Furthermore, $1/n_F$ is used to evaluate the intensity of adsorption or the surface heterogeneity of the adsorption system. $1/n_F < 1$ indicates a Langmuir adsorption condition, whereas $1/n_F > 1$ indicated a cooperative adsorption process [12, 22, 28]. The results, $n_F = 1.15$ and $1/n_F = 0.866$ (Table 9), revealed that nitrate adsorption from groundwater by granular activated carbon prepared from coconut husk is a physical process and the experimental data are best described by the Langmuir isotherm. These results are consistent with the findings reported by Rahdar et al. [62] and Khan et al. [37].

Conclusions

Coconut husk is a suitable lignocellulosic material for preparing highly porous chemically activated carbon with S_{BET} surface area of 1120 m^2/g and micropore volume of 0.39 cm^3/g. The batch experimental results showed that adsorption capacity of the coconut husk granular activated carbon (at adsorbent dose of 0.5 g/100 mL) at equilibrium increased from 0.1 mg/g to about 6.0 mg/g when the initial nitrate concentration in groundwater was increased from 10 to 150 mg/L with a corresponding equilibration time of 6 and 5 h, respectively. The adsorption process mechanism follows a Langmuir monolayer isotherm and it best fitted the pseudo-second order kinetic model. The occurrence of instantaneous adsorption of nitrate ion onto the surface of the granular activated carbon in this study was more favorable at higher initial groundwater nitrate concentrations ($0 < R_L < 1$). About 92.5% nitrate removal was achieved for 150 mg/L initial nitrate concentration, 0.5 g/50 mL adsorbent dose, and contact time of 6.25 h. The results from the model showed that the major non-linear interaction effects of process parameters on nitrate removal efficiency from groundwater were due to the adsorbent dose (46.52%) and the initial nitrate concentration (20.56%) of the groundwater.

The results from this study clearly proves that GAC made from coconut husk with a high surface area and porosity is reliable and efficient for nitrate removal from groundwater. In the future, column studies should be carried out in order to determine the continuous performance of K_2CO_3 treated GAC under different process conditions. Additionally, the stability, regeneration potential, environmental assessment and cost analysis of the K_2CO_3 treated GAC should be assessed for applying this technology for large-scale water treatment systems. Following repeated cycles of adsorption–desorption, as a resource conservation strategy, the nitrate-saturated adsorbents can be employed as nitrate-rich soil supplements to enhance the crop productivity.

Supplementary Information The online version contains supplementary material available at https://doi.org/10.1007/s43393-022-00108-5.

Acknowledgements The authors would like to thank IHE Delft, The Netherlands and the Netherlands Fellowship Programme (NFP) for providing an MSc scholarship for the Joint AIT and UNESCO-IHE Master in Environmental Technologies for Sustainable Development (ETSuD). The authors are grateful to the School of Environment, Resources and Development (AIT, Bangkok) for providing infrastructural support to carry out this research.

References

1. Abascal E, Gómez-Coma L, Ortiz I, Ortiz A. Global diagnosis of nitrate pollution in groundwater and review of removal technologies. Sci Total Environ. 2021;810: 152233.
2. Acharya S, Sharma SK, Khandegar V. Nitrate removal from groundwater by electrocoagulation: process optimization through response surface method. J Hazard Toxic Radioact Waste. 2021;25(3):04021014.
3. Adebowale T, Surapaneni A, Faulkner D, McCance W, Wang S, Currell M. Delineation of contaminant sources and denitrification using isotopes of nitrate near a wastewater treatment plant in peri-urban settings. Sci Total Environ. 2019;651(2):2701–11.
4. Afkhami A, Madrakian T, Karimi Z. The effect of acid treatment of carbon cloth on the adsorption of nitrite and nitrate ions. J Hazard Mater. 2006;144(1–2):427–31.
5. Ahmed MB, Zhou JL, Ngo HH, Guo W, Chen M. Progress in the preparation and application of modified biochar for improved contaminant removal from water and wastewater. Bioresour Technol. 2016;214:836–51.
6. APHA (American Public Health Association). Standard methods for examination of water and wastewater. 23rd ed. Washington, DC: APHA; 2015.
7. Archana A, Thibodeau B, Geeraert N, Xu MN, Kao S-J, Baker DM. Nitrogen sources and cycling revealed by dual isotopes

of nitrate in a complex urbanized environment. Water Res. 2018;142(1):459–70.
8. Barton RR. Response surface methodology. In: Gass SI, Fu MC, editors. Encyclopedia of operations research and management science. Boston: Springer; 2013.
9. Battas A, El Gaidoumi A, Ksakas A, Kherbeche A. Adsorption study for the removal of nitrate from water using local clay. Sci World J. 2019. https://doi.org/10.1155/2019/9529618.
10. Berkessa YW, Mereta SD, Feyisa FF. Simultaneous removal of nitrate and phosphate from wastewater using solid waste from factory. Appl Water Sci. 2019;9:28.
11. Bhatnagar A, Sillanpää M. A review of emerging adsorbents for nitrate removal from water. Chem Eng J. 2011;168:493–504.
12. Bhatnagar A, Ji M, Choi YH, Jung W, Lee SH, Kim SJ, Kang JW. Removal of nitrate from water by adsorption onto zinc chloride treated activated carbon. Sep Sci Technol. 2008;43(4):886–907.
13. Bolivar-Telleria M, Turbay C, Favarato L, Carneiro T, de Biasi RS, Fernandes AAR, Santos MCA, Fernandes PMB. Second-generation bioethanol from coconut husk. Biomed Res Int. 2018;2018:4916497.
14. Cameira MR, Rolim J, Valente F, Mesquita M, Dragosit U, Cordovil CMDS. Translating the agricultural N surplus hazard into groundwater pollution risk: implications for effectiveness of mitigation measures in nitrate vulnerable zones. Agr Ecosyst Environ. 2020;306: 107204.
15. Candioti LV, De Zan MM, Cámara MS, Goicoechea HC. Experimental design and multiple response optimization. Using the desirability function in analytical methods development. Talanta. 2014;124:123–38.
16. Cazetta AL, Vargas AM, Nogami EM, Kunita MH, Guilherme MR, Martins AC, Almeida VC. NaOH-activated carbon of high surface area produced from coconut shell: kinetics and equilibrium studies from the methylene blue adsorption. Chem Eng J. 2011;174(1):117–25.
17. Din ATM, Hameed BH, Ahmad AL. Batch adsorption of phenol onto physiochemical-activated coconut shell. J Hazard Mater. 2009;161(2–3):1522–9.
18. Ding L, Song J, Huang D, Lei J, Li X, Sun J. Simultaneous removal of nitrate and hexavalent chromium in groundwater using indigenous microorganisms enhanced by emulsified vegetable oil: Interactions and remediation threshold values. J Hazard Mater. 2021;406: 124708.
19. El Ouardi M, Qourzal S, Alahiane S, Assabbane A, Douch J. Effective removal of nitrates ions from aqueous solution using new clay as potential low-cost adsorbent. J Encapsul Adsorpt Sci. 2015;5(4):178–90.
20. Espejo-Herrera N, Gràcia-Lavedan E, Boldo E, et al. Colorectal cancer risk and nitrate exposure through drinking water and diet. Int J Cancer. 2016;139(2):334–46.
21. Fidel RB, Laird DA, Spokas KA. Sorption of ammonium and nitrate to biochars is electrostatic and pH dependent. Sci Rep. 2018;8:17627.
22. Foo KY, Hameed BH. Insights into the modeling of adsorption isotherm systems. Chem Eng J. 2010;156(1):2–10.
23. Golestanifar H, Asadi A, Alinezhad A, Haybati B, Vosoughi M. Isotherm and kinetic studies on the adsorption of nitrate onto nanoalumina and iron-modified pumice. Desalin Water Treat. 2016;57(12):5480–7.
24. Gonce N, Voudrias EA. Removal of chlorite and chlorate ions from water using granular activated carbon. Water Res. 1994;28(5):1059–69.
25. Gurten II, Meryem O, Yagmur E, Aktas Z. Preparation and characterization of activated carbon from waste tea using K_2CO_3. Biomass Bioenergy. 2012;37:73–81.
26. Gutiérrez M, Biagioni RN, Alarcón-Herrera MT, Rivas-Lucero BA. An overview of nitrate sources and operating processes in arid and semiarid aquifer systems. Sci Total Environ. 2018;624:1513–22.
27. Hameed S, Sharma A, Pareek V, Wu H, Yu Y. A review on biomass pyrolysis models: kinetic, network and mechanistic models. Biomass Bioenergy. 2019;123:104–22.
28. Hameed BH, Tan IAW, Ahmad AL. Adsorption isotherm, kinetic modeling and mechanism of 2, 4, 6-trichlorophenol on coconut husk-based activated carbon. Chem Eng J. 2008;144(2):235–44.
29. Hayashi J, Horikawa T, Takeda I, Muroyama K, Ani FN. Preparing activated carbon from various nutshells by chemical activation with K_2CO_3. Carbon. 2002;79(13):2381–6.
30. Hernández-Montoya V, García-Servin J, Bueno-López JI. Thermal treatments and activation procedures used in the preparation of activated carbons, lignocellulosic precursors used in the synthesis of activated carbon-characterization techniques and applications in the wastewater treatment. In: Montoya VH, editor. Lignocellulosic precursors used in the synthesis of activated carbon, vol. 2. London: InTech; 2012. p. 19–13.
31. Ho Y-S, McKay G. Pseudo-second order model for sorption processes. Process Biochem. 1999;34:451–65.
32. Hu S, Jess A, Xu M. Kinetic study of Chinese biomass slow pyrolysis: comparison of different kinetic models. Fuel. 2007;86(17–18):2778–88.
33. Hu S, Wu Y, Zhang Y, Zhou B, Xu X. Nitrate removal from groundwater by heterotrophic/autotrophic denitrification using easily degradable organics and nano-zero valent iron as co-electron donors. Water Air Soil Pollut. 2018;229(3):56–65.
34. Huno SKM, Rene ER, van Hullebusch ED, Annachhatre AP. Nitrate removal from groundwater: a review of natural and engineered processes. J Water Supply Res Technol AQUA. 2018;67(8):885–902.
35. Januszewicz K, Kazimierski P, Klein M, Kardasé D, Łuczak J. Activated carbon produced by pyrolysis of waste wood and straw for potential wastewater adsorption. Materials. 2020;13:2047.
36. Jones RR, Weyer PJ, DellaValle CT, et al. Nitrate from drinking water and diet and bladder cancer among postmenopausal women in Iowa. Environ Health Perspect. 2016;124:1751–8.
37. Khan MA, Ahn YT, Kumar M, Lee W, Min B, Kim G, Jeon BH. Adsorption studies for the removal of nitrate using modified lignite granular activated carbon. Sep Sci Technol. 2011;46(16):2575–84.
38. Khan SN, Yasmeen T, Riaz M, Arif MS, Rizwan M, Ali S, Tariq A, Jessen S. Spatio-temporal variations of shallow and deep well groundwater nitrate concentrations along the Indus River floodplain aquifer in Pakistan. Environ Pollut. 2019;253:384–92.
39. Lagergren S. About the theory of so-called adsorption of soluble substances. Kungliga Svenska Vetenskapsakademiens Handlingar. 1898;24:1–39.
40. Jones RR, Weyer PJ, DellaValle CT, et al. Nitrate from drinking water and diet and bladder cancer among postmenopausal women in Iowa. Environ Health Perspect. 2016;124:1751–8.
41. Lau YK, Yeong YF. Optimisation of nitrate removal from aqueous solution by amine functionalized MCM-41 using response surface methodology. Procedia Eng. 2016;148:239–1246.
42. Lee S, Fasina O. TG-FTIR analysis of switchgrass pyrolysis. J Anal Appl Pyrol. 2009;86:39–43.
43. Liu J, Cheng X, Zhang Y, Wang X, Zou Q, Fua L. Zeolite modification for adsorptive removal of nitrite from aqueous solutions. Microporous Mesoporous Mater. 2017;252:179–87.
44. Liu Y, Zhang X, Wang J. A critical review of various adsorbents for selective removal of nitrate from water: structure, performance and mechanism. Chemosphere. 2022;291(1): 132728.
45. Madan SS, Wasewar KL, Kumar CR. Optimization of adsorptive removal of α-toluic acid by CaO_2 nanoparticles using response surface methodology. Resour Effic Technol. 2017;3(3):329–36.

46. Mandal S, Mahapatra SS, Sahu MK, Patel RK. Artificial neural network modelling of As (III) removal from water by novel hybrid material. Process Saf Environ Prot. 2015;93:249–64.
47. Martins AP, Sanches RA. Assessment of coconut fibers for textile applications. Matéria (Rio de Janeiro). 2019;24(3):12428.
48. Mazarji M, Aminzadeh B, Baghdadi M, Bhatnager A. Removal of nitrate from aqueous solution using modified granular activated carbon. J Mol Liq. 2017;233:139–48.
49. Mazlan MAF, Uemura Y, Osman NB, Yusup S. Characterizations of bio-char from fast pyrolysis of meranti wood sawdust. J Phys Conf Ser. 2015;622(1):12054.
50. McKee DW. Mechanisms of alkali metal catalyzed gasification of carbon. Fuel. 1983;62(2):170–5.
51. Meftah T, Zerafat MM. Nitrate removal from drinking water using organo-silane modified natural nano-zeolite. Int J Nanosci Nanotechnol. 2016;12(4):223–32.
52. Mehdinejadiani B, Amininasa SM, Manhooei L. Enhanced adsorption of nitrate from water by modified wheat straw: equilibrium, kinetic and thermodynamic studies. Water Sci Technol. 2019;79(2):302–13.
53. Mishra PC, Islam M, Patel RK. Removal of nitrate-nitrogen from aqueous medium by adsorbents derived from pomegranate rind. Desalin Water Treat. 2014;52(28–30):5673–80.
54. Nandan BJ, Abdul APK. Pollution indicators of coconut husk retting areas in the kayals of Kerala. Int J Environ Stud. 1995;47(1):19–25.
55. Nandan BS. Retting of coconut husk-a unique case of water pollution on the South West coast of India. Int J Environ Stud. 1997;52(1–4):335.
56. Nunell GV, Fernandez ME, Bonelli PR, Cukierman AL. Nitrate uptake improvement by modified activated carbons developed from two species of pine cones. J Colloid Interface Sci. 2015;440:102–8.
57. Öztürk N, Köse TE. Boron removal from aqueous solutions by ion-exchange resin: batch studies. Desalination. 2008;227(1–3):233–40.
58. Pennino MJ, Compton JE, Leibowitz SG. Trends in drinking water nitrate violations across the United States. Environ Sci Technol. 2017;51(22):13450–60.
59. Prahas D, Kartika Y, Indraswati N, Ismadji S. Activated carbon from jackfruit peel waste by H_3PO_4 chemical activation: pore structure and surface chemistry characterization. Chem Eng J. 2008;140(1–3):32–42.
60. Priyankashri KN, Surendra HJ. Low-cost bench scale community level water treatment system and adsorption method for removal of nitrate from groundwater. Sustain Water Resour Manag. 2020;6:103.
61. Qiu H, Herong G, Lin C, Zhenggao P, Biao L. Hydrogeochemical characteristics and water quality assessment of shallow groundwater: a case study from Linhuan coal-mining district in northern Anhui Province, China. Water Supply. 2019;19(5):1572–8.
62. Rahdar S, Pal K, Mohammadi L, Rahdar A, Goharniya Y, Samani S, Kyzas GZ. Response surface methodology for the removal of nitrate ions by adsorption onto copper oxide nanoparticles. J Mol Struct. 2021;1231: 129686.
63. Rajic L, Berroa D, Gregor S, Elbakri S, MacNeil M, Alshawabkeh AN. Electrochemically-induced reduction of nitrate in aqueous solution. Int J Electrochem Sci. 2017;12(7):5998–6009.
64. Ren H-J, Su Y, Wang C, Hou Z-N, Zhou Y, Zhou R. Application of response surface methodology to optimize nitrate removal at low temperature by aerobic denitrificator *Pseudomonas* strain An-1. Water Environ J. 2017;32(2):235–41.
65. Riedel T, Kübeck C, Quirin M. Legacy nitrate and trace metal (Mn, Ni, As, Cd, U) pollution in anaerobic groundwater: quantifying potential health risk from "the other nitrate problem." Appl Geochem. 2022;139: 105254.
66. Serio F, Miglietta PP, Lamastra L, Ficocelli S, Intini F, Leo FD, Donno AD. Groundwater nitrate contamination and agricultural land use: a grey water footprint perspective in Southern Apulia Region (Italy). Sci Total Environ. 2018;645:1425–31.
67. Singh G, Rishi MS, Herojeet R, Kaur L, Sharma K. Evaluation of groundwater quality and human health risks from fluoride and nitrate in semi-arid region of northern India. Environ Geochem Health. 2019;42:1833–62.
68. Singh KP, Malik A, Sinha S, Ojha P. Liquid-phase adsorption of phenols using activated carbons derived from agricultural waste material. J Hazard Mater. 2008;150(3):626–41.
69. Sorlini S, Biasibetti M, Collivignarelli MC, Crotti BM. Reducing the chlorine dioxide demand in final disinfection of drinking water treatment plants using activated carbon. J Environ Technol. 2015;36(12):1499–509.
70. Sowmya A, Meenakshi S. Effective removal of nitrate and phosphate anions from aqueous solutions using functionalized chitosan beads. Desalin Water Treat. 2014;52(13–15):2583–93.
71. Suman S, Gautam S. Pyrolysis of coconut husk biomass: analysis of its biochar properties. Energy Sources Part A Recov Util Environ Eff. 2017;39(8):761–7.
72. Tan IAW, Ahmad AL, Hameed BH. Preparation of activated carbon from coconut husk: optimisation removal of 2,4,6-trichlorophenol using response surface methodology. J Hazard Mater. 2008;153(1–2):709–17.
73. Trubetskaya A, Timko MT, Umeki K. Prediction of fast pyrolysis products yields using lignocellulosic compounds and ash contents. Appl Energy. 2020;257: 113897.
74. Siling L, Binghua L, Huijuan L, Weixiao Q, Yunfeng Y, Gang Y, Jiuhui Q. The biogeochemical responses of hyporheic groundwater to the long-run managed aquifer recharge: Linking microbial communities to hydrochemistry and micropollutants. J Hazard Mater. 2022;431:128587.
75. Ward MH, Jones RR, Brender JD, de Kok TM, Weyer PJ, Nolan BT, Villanueva CM, van Breda SG. Drinking water nitrate and human health: an updated review. Int J Environ Res Public Health. 2018;15(7):1557.
76. WHO (World Health Organization).Guidelines for drinking-water quality (4th ed., p. 564). 2011. www.whqlibdoc.who.int/publications/2011/9789241548151_eng.pdf
77. Widory D, Petelet-Giraud E, Négrel P, Ladouche B. Tracking the sources of nitrate in groundwater using coupled nitrogen and boron isotopes: a synthesis. Environ Sci Technol. 2005;39(2):539–48.
78. Wolfe AH, Patz JA. Reactive nitrogen and human health: acute and long-term implications. Ambio J Hum Environ. 2002;31(2):120–5.
79. Wright PR, McMahon PB. Sampling and analysis plan for the characterization of groundwater quality in two monitoring wells near Pavillion, Wyoming: U.S. Geological Survey Open-File Report 2012–1197, 90 (2012)
80. Yang L, Yang M, Xu P, Zhao X, Bai H, Li H. Characteristics of nitrate removal from aqueous solution by modified steel slag. Water. 2017;9:757.
81. Yazdi F, Anbia M, Salehi S. Characterization of functionalized chitosan-clinoptilolite nanocomposites for nitrate removal from aqueous media. Int J Biol Macromol. 2019;130:545–55.
82. Yu J, Paterson N, Blamey J, Millan M. Cellulose, xylan and lignin interactions during pyrolysis of lignocellulosic biomass. Fuel. 2017;191:140–9.
83. Zareie H, Yazdani F, Mokhtarani B. Removal of water nitrate using modified Purolite A520E resin, synthesis and experimental design. Mater Chem Phys. 2022;285: 126098.

84. Zhang Q, Qian H, Xu P, Li W, Feng W, Liu R. Effect of hydrogeological conditions on groundwater nitrate pollution and human health risk assessment of nitrate in Jiaokou Irrigation District. J Clean Prod. 2021;298: 126783.
85. Zhao F, Xin J, Yuan M, Wang L, Wang X. A critical review of existing mechanisms and strategies to enhance N_2 selectivity in groundwater nitrate reduction. Water Res. 2022;209: 117889.
86. Zhao S, Liu M, Zhao L, Zhu L. Influence of interactions among three biomass components on the pyrolysis behavior. Ind Eng Chem Res. 2018;57:5241–9.

Authors and Affiliations

Solomon K. M. Huno[1,2] · Jewel Das[3,4] · Eric D. van Hullebusch[1,5] · Ajit P. Annachhatre[2,6] · Eldon R. Rene[1]

✉ Eldon R. Rene
e.raj@un-ihe.org

[1] Pollution Prevention and Resource Recovery Chair Group, Department of Water Supply, Sanitation and Environmental Engineering, IHE Delft Institute of Water Education, P.O. Box 3015, 2601 DA Delft, The Netherlands

[2] Environmental Engineering and Management, Department of Environment, Energy and Climate Change, School of Environment, Resource and Development, Asian Institute of Technology, 58 Moo 9, Km. 42, Paholyothin Highway, P.O. Box 4, Klong Luang 12120, Pathum Thani, Thailand

[3] National University of Ireland Galway, University Road, Galway H91 TK33, Ireland

[4] Bangladesh Council of Scientific and Industrial Research (BCSIR), BCSIR Laboratories Chattogram, Chattogram 4220, Bangladesh

[5] Université Paris Cité, Institut de Physique du Globe de Paris, CNRS, F-75005 Paris, France

[6] School of Engineering, Indian Institute of Technology Mandi, A4-209, Mandi, Himachal Pradesh 175001, India